NUCLEAR THEORY, Vol. 39 (2022)
eds. M. Gaidarov, N. Minkov, Heron Press, Sofia

Study of Structural and Decay Properties of Even-Even Pb Isotopes within CDF Theory

M. El Adri, **M. Oulne**

High Energy Physics and Astrophysics Laboratory, Department of Physics, Faculty of Sciences Semlalia, Cadi Ayyad University, P.O.B. 2390, Marrakesh, Morocco

Abstract. Numerical calculations of the structural and decay ground state properties of the even-even isotopes of lead Pb are presented. Such calculations are based on the relativistic Hartree-Bogoliubov method using the DD-ME2 and DD-PC1 effective interactions. Predictions for binding energies, two-neutron separation energies, two-neutron gaps, pairing energies, charge radii and α-decay properties are presented and discussed. The study shows that the relativistic Hartree-Bogoliubov theory is able to describe, with high accuracy, the ground state properties of Pb isotopes. In addition, the well-known number magic N=126 is reproduced and the N=184 is established as as candidate magic number for neutron in the exotic region.

keywords : Relativistic Hartree-Bogoliubov method; Pb isotopes; Binding energy; two-neutron separation energies; two-neutron gaps; pairing energy; α-decay properties

1 Introduction

Energy density functionals (EDF) provide an accurate description of ground-state properties and collective excitations of atomic nuclei, from relatively light systems to superheavy nuclei, and from the valley of $\beta-$stability to the particle drip-lines [1, 2]. A particular class of EDF structure models are those based on relativistic (covariant) energy density functionals. These models have been successfully applied to the analysis of a variety of nuclear structure phenomena, and the level of accuracy has reached a level comparable to the non-relativistic HartreeFockBogoliubov approach based on Skyrme functionals [3] or Gogny effective interactions [4]. Here we have studied the features of even-even Pb isotopes using the program package DIRHB for the solution of the stationary relativistic HartreeBogoliubov equations for eveneven nuclei with axially symmetric quadrupole deformation [5].

The paper is organized as follows: Section 2 shortly summarizes the approaches that we have used to do our calculations. In Section 3, numerical tests as well as the input details and the interactions used in calculations are presented. The obtained results are analyzed and discussed in Section 4. Finally, the main conclusions and outlook are given in Section 5.

2 Theoretical Framework

Covariant Density Functional Theory (CDFT), also often labelled as relativistic Hartree-Bogoliubov (RHB) theory, is a microscopic theoretical tool that can be used to describe the entire nuclear chart with success. In the present work, we have employed two classes of relativistic Hartree-Bogoliubov theories. The first one is the DD-PC model [6,7] which is characterised by a zero-range interaction and the second one is the DD-ME model [5] which uses a finite interaction range. A brief description of these models is given in the following subsections.

2.1 The density-dependent point-coupling

The effective Lagrangian density of DD-PC model is defined by [6]

$$\begin{aligned}\mathcal{L} = \bar{\psi}(i\gamma.\partial - m)\psi - \frac{1}{2}\alpha_S(\rho)(\bar{\psi}\psi)(\bar{\psi}\psi) \\ - \frac{1}{2}\alpha_V(\rho)(\bar{\psi}\gamma^\mu\psi)(\bar{\psi}\gamma_\mu\psi) - \frac{1}{2}\alpha_{TV}(\rho)(\bar{\psi}\vec{\tau}\gamma^\mu\psi)(\bar{\psi}\vec{\tau}\gamma_\mu\psi) \\ - \frac{1}{2}\delta_S(\partial_\nu\bar{\psi}\psi)(\partial_\nu\bar{\psi}\psi) - e\bar{\psi}\gamma.A.\frac{1-\tau_3}{2}\psi\,. \quad (1)\end{aligned}$$

This Lagrangian contains the isoscalar-scalar interaction (σ meson) $(\bar{\psi}\psi)(\bar{\psi}\psi)$, isoscalar-vector interaction (ω meson) $(\bar{\psi}\gamma^\mu\psi)(\bar{\psi}\gamma_\mu\psi)$, isovector-vector interaction (ρ meson) $(\bar{\psi}\vec{\tau}\gamma^\mu\psi)(\bar{\psi}\vec{\tau}\gamma_\mu\psi)$ and their corresponding gradient couplings $\partial_\nu(...)\partial^\nu(...)$. It also contains the free-nucleon Lagrangian, the point-coupling interaction terms and the coupling of protons to the electromagnetic field. The derivative terms in eq. (1) account for the main effects of finite range interactions which are important for a quantitative description of nuclear density distribution. The functional form of the couplings is given by

$$\alpha_i(\rho) = a_i + (b_i + c_i x)e^{-d_i x} \qquad \text{for} \quad i = S, T, TV\,, \quad (2)$$

where $x = \rho/\rho_{sat}$ and ρ_{sat} denotes the nucleon density in units of the saturation density of symmetric nuclear matter. For more details see Ref [5].

2.2 The density-dependent meson-exchange

The basic building blocks of relativistic Hartree-Bogoliubov for DD-ME is the standard Lagrangian density with medium dependent vertice [5]

$$\begin{aligned}\mathcal{L} = \bar{\psi}\left[\gamma(i\partial - g_\omega\omega - g_\rho\vec{\rho}\,\vec{\tau} - eA) - m - g_\sigma\sigma\right]\psi \\ + \frac{1}{2}(\partial\sigma)^2 - \frac{1}{2}m_\sigma^2\sigma^2 - \frac{1}{4}\Omega_{\mu\nu}\Omega^{\mu\nu} + \frac{1}{2}m_\omega^2\omega^2 \\ - \frac{1}{4}\vec{R}_{\mu\nu}\vec{R}^{\mu\nu} + \frac{1}{2}m_\rho^2\vec{\rho}^{\,2} - \frac{1}{4}F_{\mu\nu}F^{\mu\nu} \quad (3)\end{aligned}$$

with ψ is Dirac spinor and m is the bare nucleon mass. m_σ, m_ω and m_ρ are meson masses. g_σ, g_ω and g_ρ are the coupling constants and e corresponds to the proton's charge. It vanishes for neutron. $\Omega_{\mu\nu}$, $\vec{R}^{\mu\nu}$, $F_{\mu\nu}$ denote fields tensors.

$$\Omega_{\mu\nu} = \partial^\mu \Omega^\nu - \partial^\nu \Omega^\mu \,, \tag{4}$$

$$\vec{R}^{\mu\nu} = \partial^\mu \vec{\rho}^{\,\nu} - \partial^\nu \vec{\rho}^{\,\mu} \,, \tag{5}$$

$$F_{\mu\nu} = \partial^\mu A^\nu - \partial^\nu A^\mu \,. \tag{6}$$

The coupling of the σ and ω mesons to the nucleon field reads [5]

$$g_i(\rho) = g_i(\rho_{sat}) f_i(x) \qquad \text{for} \quad i = \sigma, \omega \tag{7}$$

with the density dependence given by

$$f_i(x) = a_i \frac{1 + b_i(x + d_i)^2}{1 + c_i(x + d_i)^2} \,, \tag{8}$$

where $x = \rho/\rho_{sat}$, ρ is the baryonic density and ρ_{sat} is the baryon density at saturation in symmetric nuclear matter. In eq. (8), the parameters are not independent, but constrained as follows: $f_i(1) = 1$, $f''_\sigma(1) = f''_\omega(1)$, and $f''_i(0) = 0$. These constraints reduce the number of independent parameters for the density dependence.
In the ρ-meson case, we have an exponential density dependence

$$g_\rho(\rho) = g_\rho(\rho_{sat}) e^{-a_\rho(x-1)} \,. \tag{9}$$

The isovector channel is parametrized by $g_\rho(\rho_{sat})$ and a_ρ.

3 Numerical Details

This investigation is realized by using the relativistic Hartree-Bogoliubov (RHB) theory based on the DD-PC1 and DD-ME2 functionals and separable pairing within the DIRHB package [5], in which the RHB equations can be solved iteratively in a basis of spherical, axially symmetric or triaxial harmonic oscillator (HO).

In our calculation, we have used the finite range pairing interaction separable in coordinate space which was proposed by Tian et al. [8]. It is given in the pp-channel by

$$V^{pp}(\mathbf{r_1}, \mathbf{r_2}, \mathbf{r'_1}, \mathbf{r'_2}) = -G\delta(\mathbf{R} - \mathbf{R}')P(r)P(r') \,, \tag{10}$$

where $\mathbf{R} = \frac{1}{2}(\mathbf{r_1} + \mathbf{r_2})$ is the centre of mass, $\mathbf{r} = \mathbf{r}_1 - \mathbf{r}_2$ are the relative coordinates and $P(r)$ represents the form factor which is given by

$$P(r) = \frac{1}{(4\pi a^2)^{3/2}} e^{-\frac{r^2}{4a^2}} \tag{11}$$

The two parameters: the pairing strength G and the pairing width a have been adjusted to reproduce the density dependence of the gap at the Fermi surface. The following values: $G = 728$ MeV.fm^3 and $a = 0.6442$ fm which were determined for the D1S parametrization [8] of the Gogny force have also been used here. The numbers of Gauss-Laguerre $N_{\rm GL}$ and Gauss-Hermite $N_{\rm GH}$ mesh-points were $N_{\rm GL} = N_{\rm GH} = 48$, and the number of Gauss-Legendre mesh-points was $N_{\rm GLEG} = 80$.

It is noted that all calculations performed with the DIRHB code are carried out in a safe full anisotropic basis of $N_{\rm F} = 18$ for fermions. But for the bosons, the number of shells is fixed to $N_{\rm B} = 20$. The β_2-deformation parameter for the harmonic oscillator basis as well as for the initial Woods-Saxon potential is set to 0. The different parameter sets of used functionals, i.e. DD-ME2 and DD-PC1, are given in Table 1.

Table 1. The different parameter sets of DD-ME2 [7] and DD-PC1 [6] interactions.

Parameter		**DD-ME2** [7]	**Parameter**		**DD-PC1** [6]
m	(MeV)	939	m	(MeV)	939
m_σ	(MeV)	550.124	a_σ	(fm^2)	-10.04616
m_ω	(MeV)	783.000	b_σ	(fm^2)	-9.15042
m_ρ	(MeV)	763.00	c_σ	(fm^2)	-6.42729
m_δ	(MeV)	0.000	d_σ		1.37235
g_σ		10.5396	a_ω	(fm^2)	5.91946
g_ω		13.0189	b_ω	(fm^2)	8.86370
g_ρ		3.6836	b_ρ	(fm^2)	1.83595
g_δ		0.000	d_ρ		0.64025
a_σ		1.3881			
b_σ		1.0943			
c_σ		1.7057			
d_σ		0.4421			
e_σ		0.4421			
a_ω		1.3892			
b_ω		0.9240			
c_ω		1.4620			
d_ω		0.4775			
e_ω		0.4775			
a_ρ		0.5647			

4 Results and Discussion

4.1 Average binding energy

We have performed calculations of the average binding energies BE/A of Pb isotopes using DD-PC1 and DD-ME2 parametrizations, whose values as function of neutron number N are shown in Figure 1. From this Figure, it is seen that

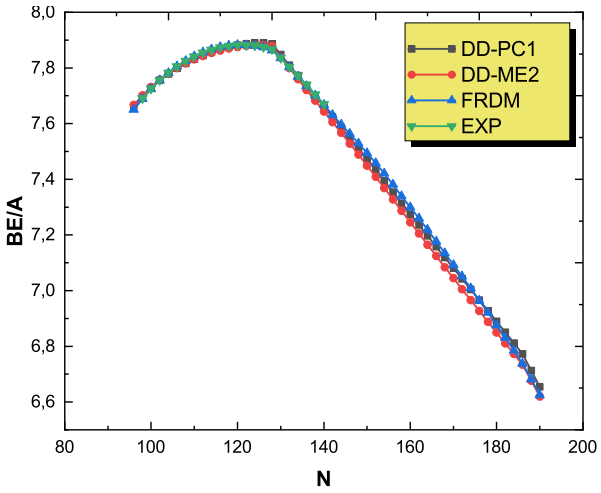

Figure 1. The average binding energies BE/A of even-even Pb isotopes calculated using DD-PC1 and DD-ME2 parametrizations. The green dotted line represent the experimental values taken from Ref. [10].

the experimental data for BE/A can be reproduced accurately by the DD-ME2 and DD-PC1 interactions and the FRDM model [9]. In the exotic region, there is a deviation between the theoretical results but it still very small. Note that the average binding energy, can give an idea about the stability of nuclei. Here the most stable nuclei – with high BE/A – are found around $N = 130$.

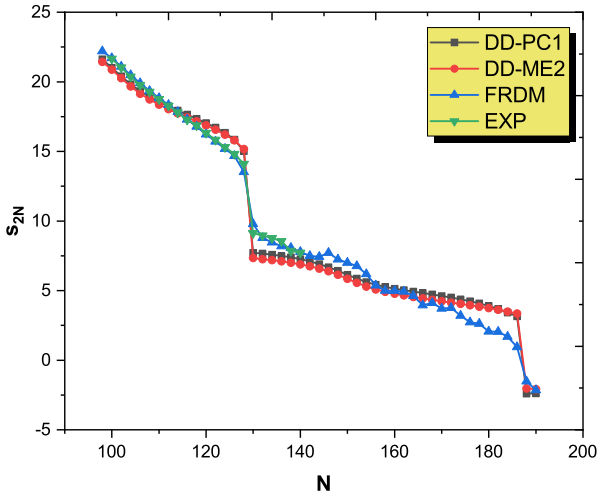

Figure 2. Same as Figure 1, but for S_{2N}.

4.2 Two-neutron separation energy

We extract the two-neutron separation energy using the calculated binding energy values BE for each interaction, which is given by the following formula:

$$S_{2n} = BE(N) - BE(N-2) \tag{12}$$

In Figure 2 we have plotted the evolution of S_{2N} as a function of N. From the experimental data as well as the theoretical models for S_{2N} versus N, we can see the shell effects at ^{206}Pb ($N = 126$) which is last neutron magic number in the valley of stability. In the exotic region, we observe, from the theoretical models, the shell effects at ^{266}Pb ($N = 184$). Therefore, this number is considered as a first number magic for neutron beyond the ^{206}Pb in the exotic region. Furthermore, the shell effects at $N = 184$ given by the DD-ME2 and DD-PC1 interactions is more evident than in the FRDM predictions.

4.3 Two-neutron shell closure

A more direct measure of the shell effect, is the two-neutron shell closure that is defined by the following expression:

$$\delta_{2n} = S_{2n}(N+2) - S_{2n}(N) \tag{13}$$

In the Figure 3, we can observe that the experimental data for δ_{2N} as well as the theoretical models show a sharp peak at N=126 and at N=184. Here, again the shell effect is more pronounced by the DD-ME2 and by DD-PC1 interactions.

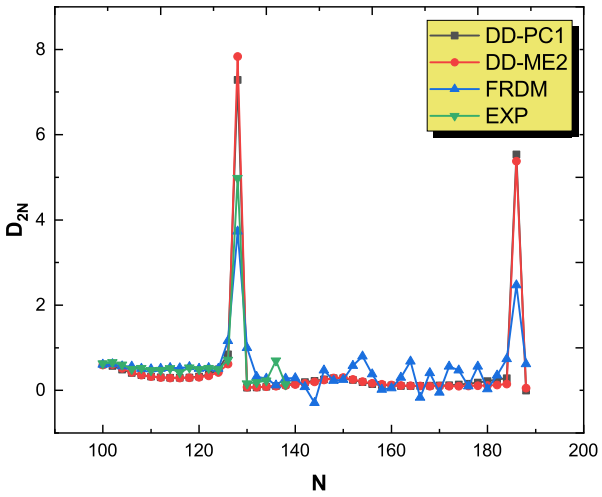

Figure 3. (Color online) Comparison between the experimental data and calculated δ_{2N} for Pb isotopes with the DD-PC1 and DD-ME2 interactions and FRDM model.

4.4 Pairing energy

In magic nuclei, the pairing effect is vanished. Thus, calculating the pairing energy of nuclei allows to detect their magicity. In Figure 4, we display the neutron pairing energy for the eveneven Pb isotopes as a function of neutron number N. So, we can observe clearly that the pairing energy vanishes exactly at N=126 and N=184 indicating a neutron shell closures for the nucleus under investigation in these positions.

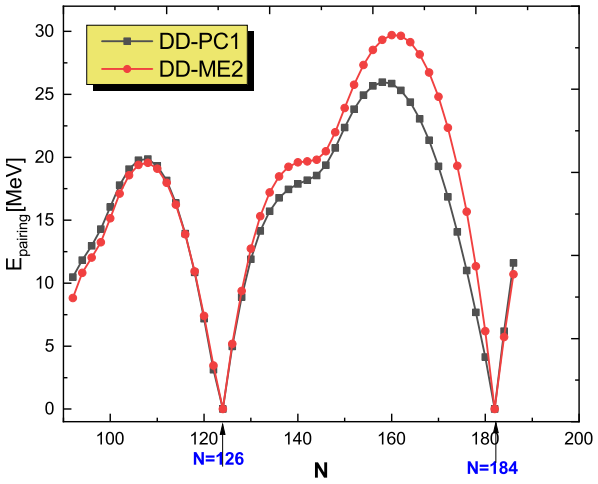

Figure 4. (The calculated neutron pairing energy in even-even Pb isotopes the DD-PC1 and the DD-ME2 sets.

4.5 Charge radii

We calculated also the charge radii of even-even Pb isotopes as a function of neutron number as displayed in the Figure 5. Observing experimental data for the charge radii and the calculated values using DD-ME2 and DD-PC1, a minimum at N=126 can be clearly seen. However, in the exotic region, the minimum appears only in DD-PC1 interaction, around N=184, where the experimental data are not available. This implies that the minimum at N=184 might depends on the used functional beyond the mean field for the exotic nuclei.

4.6 Q_α-energy

To study the decay properties for the even-even lead isotopes, we have calculated the Q_α-energy that is the energy of spontaneous α-decay. Its expression is given by the following formula:

$$Q\alpha = BE(N,Z) - BE(N-2,Z-2) - BE(2,2) \tag{14}$$

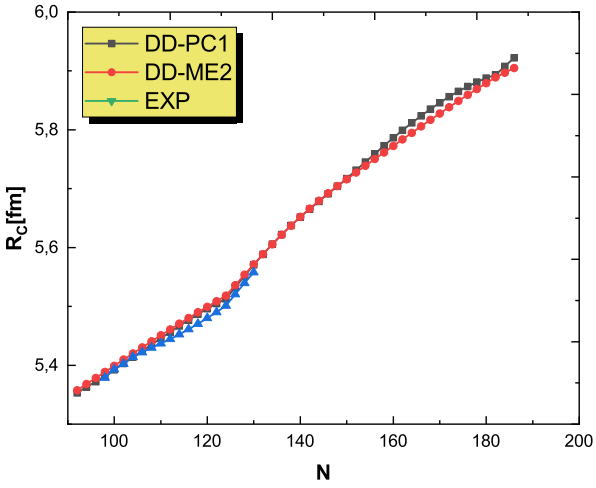

Figure 5. (Color online) Same as Figure 1, but for R_{ch}. The experimental data are taken from Ref. [11].

In Figure 6, we show this quantity of Pb isotopes predicted by DD-ME2 and DD-PC1 functionals and by FRDM model and compared with the available experimental data. So as shown in this Figure, the experimental data for the Q_α-energy and the theoritical models have almost the same trend. Furthermore, a sharp jump is observed around the well-known magic number $N = 126$ and at N=184 which can be considered as a magic number in the exotic region.

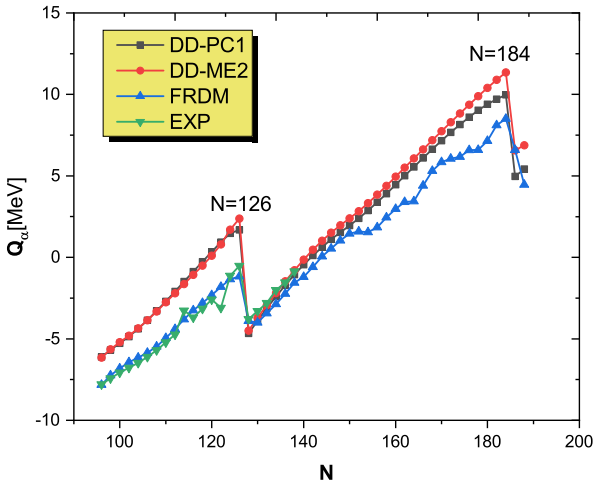

Figure 6. Same as Figure 1, but for Q_α-energy.

5 Conclusion

To sum up, even-even lead isotopes have been studied within the relativistic Hartree-Bogoliubov (RHF) using DD-PC1 and DD-ME2 functionals. Binding energies, two-neutron separation energies, two-neutron gaps, pairing energies, charge radii and α-decay energy show that $N = 126$ persists as a neutron magic number in the valley of stability and $N = 184$ is predicted to be a magic number for neutrons in the exotic region for the investigated nuclei. Furthermore, we observe that there is a good agreement between experimental data and the theoretical models.

References

[1] M. El Adri and M. Oulne, Neutron shell closure at N = 32 and N = 40 in Ar and Ca isotopes, *Eur. Phys. J. Plus.* **135** (2020) 268.

[2] M. El Adri and M. Oulne. Shell Evolution in Neutron-rich Ge, Se, Kr and Sr Nuclei within RHB Approach, *IJMPE* **29** (2020) 2050089.

[3] D. Vautherin and D.M. Brink Hartree-Fock-Bogolyubov calculations with the D1 effective interaction on spherical nuclei, *Phys. Rev. C.* **59** (1980) 626.

[4] J. Dechargé and D. Gogny *Phys. Rev. C.* **21** (1980) 1568.

[5] T. Nikšić, N. Paar, D. Vretenar et P. Ring, DIRHBA relativistic self-consistent mean-field framework for atomic nuclei, *Comput. Phys. Commun.* **185** (2014) 1808-1821

[6] T. Nikšić, D. Vretenar, and P. Ring, Relativistic nuclear energy density functionals: Adjusting parameters to binding energies, *Phys. Rev. C* **78** (2008) 034318.

[7] G.A. Lalazissis, T. Nikšić , D. Vretenar, and P. Ring, New relativistic mean-field interaction with density-dependent meson-nucleon couplings, *Phys. Rev. C* **71** (2005) 024312.

[8] Y. Tian, and Z.Y. Ma, P. Ring, A finite range pairing force for density functional theory in superfluid nuclei, *Phys. Lett. B* **676** (2009) 44.

[9] P. Mller, A.J. Sierka, T. Ichikawab, H. Sagawa, Nuclear ground-state masses and deformations: FRDM (2012) *At. Data Nucl. Data Tables* **109** (2016) 1204.

[10] M. Wang, W.J. Huang, F.G. Kondev, G. Audi, S. Naimi, The AME 2020 atomic mass evaluation (II). Tables, graphs and references, *Chin. Phys. C.* **45** (2021) 030003.

[11] I. Angeli, K.P. Marinova Table of experimental nuclear ground state charge radii: An update, *Atomic Data and Nuclear Data Tables* **99** (2013) 69-95.